Springer

Dear Author:

Please find attached the final pdf file of your contribution, which can be viewed using the Acrobat Reader, version 3.0 or higher. We would kindly like to draw your attention to the fact that copyright law is also valid for electronic products. This means especially that:

- You may not alter the pdf file, as changes to the published contribution are prohibited by copyright law.

- You may print the file and distribute it amongst your colleagues in the scientific community for scientific and/or personal use.

- You may make an article published by Springer-Verlag available on your personal home page provided the source of the published article is cited and Springer-Verlag is mentioned as copyright holder. You are requested to create a link to the published article in LINK, Springer's internet service. The link must be accompanied by the following text: The original publication is available on LINK **http://link.springer.de.** Please use the appropriate URL and/or DOI for the article in LINK. Articles disseminated via LINK are indexed, abstracted and referenced by many abstracting and information services, bibliographic networks, subscription agencies, library networks and consortia.

- You are not allowed to make the pdf file accessible to the general public, e.g. your institute/your company is not allowed to place this file on its homepage.

- Please address any queries to the production editor of the journal in question, giving your name, the journal title, volume and first page number.

Yours sincerely,

Springer-Verlag Berlin Heidelberg

Climate Dynamics (2002) 18: 475–486
DOI 10.1007/s00382-001-0189-5

B. Wang · S.I. An

A mechanism for decadal changes of ENSO behavior: roles of background wind changes

Received: 7 March 2001 / Accepted: 21 June 2001 / Published online: 4 January 2002

Abstract This study explains why a number of El Nino properties (period, amplitude, structure, and propagation) have changed in a coherent manner since the late 1970s and why these changes had almost concurred with the Pacific decadal climate shift. Evidence is presented to show that from the pre-shift (1961–1975) to the post-shift (1981–1995) epoch, significant changes in the tropical Pacific are found in the surface winds and temperature, whereas changes in the thermocline are uncertain. Numerical experiments with the Cane and Zebiak model demonstrate that the decadal changes in the surface winds qualitatively reproduce the observed coherent changes in El Nino properties. The fundamental factor that altered the model's El Nino is the decadal changes of the background equatorial winds and associated upwelling. The annual cycle is also necessary for the mean state to modulate El Nino. From the pre- to post-shift epoch, the changes in the background winds and upwelling modify the structure of the coupled mode (eastward displacement of the equatorial westerly anomalies) by reallocating anomalous atmospheric heating and SST gradient along the equator. This structural change amplifies the ENSO cycle and prolongs the oscillation period by enhancing the coupled instability and delaying transitions from a warm to a cold state or vice versa. The changes in the mean currents and upwelling reduce the effect of the zonal temperature advection while enhance that of the vertical advection; thus, the prevailing westward propagation is replaced by eastward propagation or standing oscillation. Our results suggest a critical role of the atmospheric bridge that rapidly conveys the influences of extratropical decadal variations to the tropics, and the possibility that the Pacific climate shift might have affected El Nino properties in the late 1970s by changing the background tropical winds and the associated equatorial upwelling.

B. Wang (✉) · S. I. An
International Pacific Research Center,
and Department of Meteorology School of Ocean
and Earth Science and Technology,
University of Hawaii at Manoa,
Honolulu, HI 96822, USA
E-mail: bwang@soest.hawaii.edu

1 Introduction

It has been recognized for several decades that the Southern Oscillation is non-stationary (e.g., Troup 1965). Trenberth and Shea (1987) pointed out that the Southern Oscillation was strong from 1880 to 1920 and from 1950 to 1987, and weak from the mid-1920s to 1950. The amplitude and frequency of El Nino-Southern Oscillation (ENSO) exhibit notable secular variations over the past 130 years as revealed by wavelet analysis of the Nino-3 sea surface temperature (SST) index (Gu and Philander 1995) and Southern Oscillation index (Wang and Wang 1996).

In the mid 1970s, an abrupt change in SST and large-scale winter circulation over the North Pacific was observed (Nitta and Yamada 1989; Trenberth 1990; Trenberth and Hurrell 1994). Although some aspects of this interdecadal variation, for instance, the teleconnection patterns and their influences on the extratropics, resemble features associated with El Nino episodes (Zhang et al. 1997), the interdecadal variation of the coupled system manifests itself as a mode different from the ENSO (Latif et al. 1997). Over the tropical Pacific, the climate change is better described as a shift in the background mean state of the coupled atmosphere-ocean system (Graham 1992). Concurrent changes in the frequency and intensity of El Nino and La Nina events in the 1980s and 1990s were linked to Pacific decadal variations (Trenberth and Hurrell 1994). An analysis of the 40-year (1951–1990) Comprehensive Ocean-Atmosphere Data Set (COADS) revealed that the onset and development characteristics of El Nino had experienced a significant change after the 1976–77 El Nino (Wang 1995). Changes in the behavior

of ENSO were also observed in its decay process (Shukla 1995), its tendency to be phase-locked to the annual cycle (Balmaseda et al. 1995; Mitchell and Wallace 1996), propagation of coupled anomalies (Wallace et al. 1998), and the structure of the coupled ocean-atmosphere mode (An and Wang 2000).

The decadal variability is one of the fundamental characteristics of ENSO cycles, yet the cause remains a subject of debate. While stochastic forcing and chaotic dynamics within the tropical coupled system may induce variations in the frequency and amplitude of ENSO (Zebiak and Cane 1991; Kleeman and Moore 1999), it is not clear whether they can change the structure and propagation of the coupled mode. In addition, they do not explain the simultaneous occurrence of the extratropical decadal variation and decadal variations of ENSO characteristics. Consideration of influences external to the tropical Pacific, in particular the interdecadal variability of the extratropical Pacific, becomes relevant to understanding of the cause of the recent decadal variation in ENSO cycles.

There are two issues concerning the impacts of the Pacific decadal oscillation on ENSO. One is how the extratropical decadal variations change the background state of the coupled ocean-atmosphere system over the tropical Pacific. The other is how the variation of the tropical background state modulates ENSO.

Concerning the tropical-extratropical linkage, Kleeman et al. (1999) have reviewed two major hypotheses. The first is an oceanic teleconnection. McCreary and Lu (1994) and Liu et al. (1994) have demonstrated that a large portion of the equatorial eastward undercurrent water originates in the subduction zones of the northern and southern subtropics. Thus, the water mass subducted in the subtropics might eventually affect the eastern Pacific SST. Gu and Philander (1997) proposed that ENSO atmospheric teleconnection induces subtropical and midlatitude SST anomalies of the opposite sign to the equatorial SST anomalies. These subtropical temperature anomalies can then be subducted into the thermocline and advected on the main thermocline to the equator and feedback to ENSO. Observational analysis and numerical experiments with ocean general circulation models (Schneider et al. 1999; Nonaka et al. 2000) indicate that the subsurface advective process from the midlatitudes to the tropics is ineffective in changing the equatorial subsurface thermal structure. Kleeman et al. (1999) found, based on their hybrid intermediate coupled model experiments, that the decadal oscillation originating in the midlatitudes may affect the equatorial SST through heat transport changes in the upper branch of the subtropical cell. The latter is associated with surface wind variation and serves as a driving force of the North Pacific subtropical cell. The second hypothesis is based on an atmospheric teleconnection proposed by Barnett et al. (1999) and Pierce et al. (2000), in which the decadal wind variability generated in the midlatitudes extends into the tropics and forces the tropical ocean circulation. The atmospheric teleconnection hypothesis is appealing in the sense that the timing of the decadal changes in the extratropical circulation was nearly concurrent with the shift in the tropical Pacific background state and changes in ENSO properties. However, this idea has been lacking details and thus not properly understood as it should be.

To explain how the tropical background state modulates ENSO, two lines of thinking have been offered. One is through changes in the surface winds and temperature. Wang (1995) found that after the late 1970s, a decadal warming has occurred near the equatorial dateline, extending northeastward and southeastward into the subtropical eastern Pacific. This warming pattern, on the one hand, induces anomalous equatorial westerlies in the western Pacific; on the other hand, it enhances the southeast trades. The former facilitates initiation of ENSO warming in the central Pacific while the latter prohibits warming off the South American coast, resulting in onset and propagation patterns differing from those of the canonical warm event derived by Rasemusson and Carpenter (1982) using observations before 1978. Another idea proposed by Gu and Philander (1995) emphasizes the role of secular changes in the equatorial thermocline on ENSO. It is known that ENSO-like oscillations in intermediate coupled models are sensitive to the specified basic states of the ocean thermal structure (e.g., Anderson and McCreary 1985; Zebiak and Cane 1987; Kirtman and Schopf 1998; Latif et al. 1997). However, the precise processes by which the background state influences ENSO properties were not methodically addressed.

Two critical questions have not been previously addressed: why do a number of ENSO properties change in a coherent manner and why have these changes concurred with the Pacific decadal climate shift? We focus on addressing these questions. Our strategy is to compare two contrasting periods before and after the Pacific climate shift, because the data are most reliable and because both the decadal change and ENSO property change are pronounced. To elaborate on the impacts of the Pacific decadal climate shift on ENSO, a sequence of questions must be addressed: what properties of ENSO have changed since the late 1970s? What changes have happened in the background state of the tropical Pacific in association with the Pacific decadal climate shift? Can these observed changes in the background state lead to the observed changes of ENSO in coupled ocean-atmosphere models? If so, which aspects of the background states most effectively influence ENSO, and how? Sections 2 through 6 are aimed at addressing the above questions. Section 7 discusses the uncertainties involved in this study. The last section presents a summary.

2 Changes of ENSO properties before and after the late 1970s

The dominant ENSO oscillation period increased from 2–3 years during 1961–1975 to 4–6 years during 1980–1995 (Gu and

Philander 1995; Wang and Wang 1996). When the oscillation period increases, the amplitude of ENSO tends to increase as well (see Fig. 1 of An and Wang 2000). Observations also indicate that the ENSO frequency change after the late 1970s was accompanied by a significant change in the propagation and structure of the dominant coupled ENSO mode. During the 1960s and 1970s the warm SST anomalies expanded westward from the South American coast into the central equatorial Pacific (Rasmusson and Carpenter 1982); after 1980, the warm SST anomalies propagated eastward across the basin from the central Pacific or developed concurrently in the central and eastern Pacific (Wallace et al. 1998).

In comparison with the faster oscillation occurring during 1961–1975, the structure of the dominant coupled mode during 1981–1995 shows an eastward displacement of the equatorial westerly anomalies with respect to the eastern Pacific positive SST anomalies (An and Wang 2000). To verify this result and to further examine possible changes in the ocean thermocline, we used SST and subsurface temperature data assimilated by Carton et al. (2000) using the Simple Ocean Data Assimilation (SODA data) package. A joint singular value decomposition (JSVD) method, a useful tool to detect coupled structures among multiple variables, was used to derive the structure of the dominant ENSO mode for the 1961–1975 and 1981–1995 periods separately. Figure 1a compares the zonal wind stress, zonal SST gradient and the zonal gradient of the thermocline depth anomaly along the equator (average of 5°S-5°N) for the dominant JSVD modes derived for the two epochs. The patterns of the zonal SST gradient, zonal wind stress, and the zonal thermocline slope all exhibit a systematic and dynamically coherent eastward displacement (by about 15° longitude) during 1981–1995.

It is clear that not only the frequency and amplitude of ENSO but also the structure and propagation of the coupled ENSO mode have changed. Both aspects call for explanation. In fact, we will show that the change of oscillation period and amplitude is intrinsically linked to changes in the structure of the coupled mode.

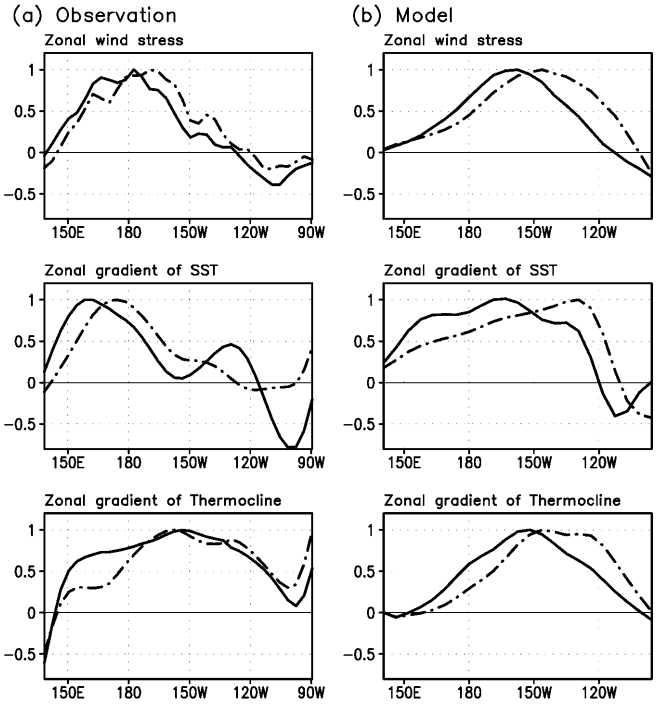

Fig. 1 **a** The observed *(left panel)* and **b** model simulated *(right panel)* equatorial distribution of zonal wind stress, zonal gradients of SST and thermocline depth anomaly. The observed (simulated) patterns were derived by normalizing the loadings of the principal joint-SVD mode derived from SODA (the CZ model outputs) for the periods of 1961–1975 *(solid line)* and 1981–1995 *(dot-dashed line)*, respectively. SODA stands for Simple Ocean Data Assimilation (Carton et al. 2000). The thermocline depth was estimated following the definition in Wang et al. (2000a)

3 Changes of the mean state in the tropical Pacific in the late 1970s

To describe secular changes in the mean states of the tropical Pacific between 1961–1975 and 1981–1995, we focus on variables that control ENSO dynamics, which, in the CZ model, include surface zonal and meridional winds (U, V) and associated divergence (DIV), sea surface temperature (SST), thermocline depth (H), and the vertical temperature difference across the surface layer base ($d\bar{T}/dz$). The surface layer currents (u, v) of the basic state and associated upwelling (w) are determined from the surface wind stress and ocean model dynamics.

The datasets used to detect decadal changes in the surface winds, SST, and thermocline include the Florida State University (FSU) pseudo wind stress (Kubota and O'Brien 1988; Shriver and O'Brien 1995), the surface winds compiled by da Silva (da Silva et al. 1994), the National Center for Environmental Prediction (NCEP) reconstructed SST (Reynolds and Smith 1994; Smith et al. 1996), and the Levitus ocean temperature data (Levitus et al. 1994; Levitus and Boyer 1994).

Figure 2a shows that the changes in mean surface wind stress from the 1961–1975 to the 1981–1995 period are characterized by anomalous westerlies in the equatorial western Pacific (west of 160°W) and easterlies in the equatorial eastern Pacific (east of 160°W), resulting in a convergence in the central Pacific around 160°W and 7°S and a minor convergence region in the equatorial eastern Pacific (Fig. 2a). These equatorial wind anomalies, which are associated with trade wind anomalies in both hemispheres, are commonly seen in both the FSU and da Silva's data sets. Over the tropical Pacific, the mean SST during 1981–1995 was higher than that during the 1961–1975 period (Fig. 2a). The estimated increase exceeds 0.5°C over the equatorial central Pacific and the southeastern tropical Pacific.

The annual cycles of the surface wind stress, in which the annual mean has been removed, also show decadal changes (Fig. 3). The winds reverse their directions between summer and winter primarily in the western Pacific, indicating that the monsoon flows intensify after the late 1970s. This is consistent with the increased convective variability over the Philippine Sea after the late 1970s (Wang et al. 2001b). The corresponding changes in the seasonal departure of SST are found in the South Pacific convergence zone and the North Pacific around (10°N, 180°E) (Fig. 3). The statistical significance is considerably lower than that in the annual mean fields. Note that the wind stress changes shown in Figs. 2a and 3 are generally consistent with the anomalous SST patterns shown in Figs. 2a and 3 in the sense that the surface winds converge into regions of warm

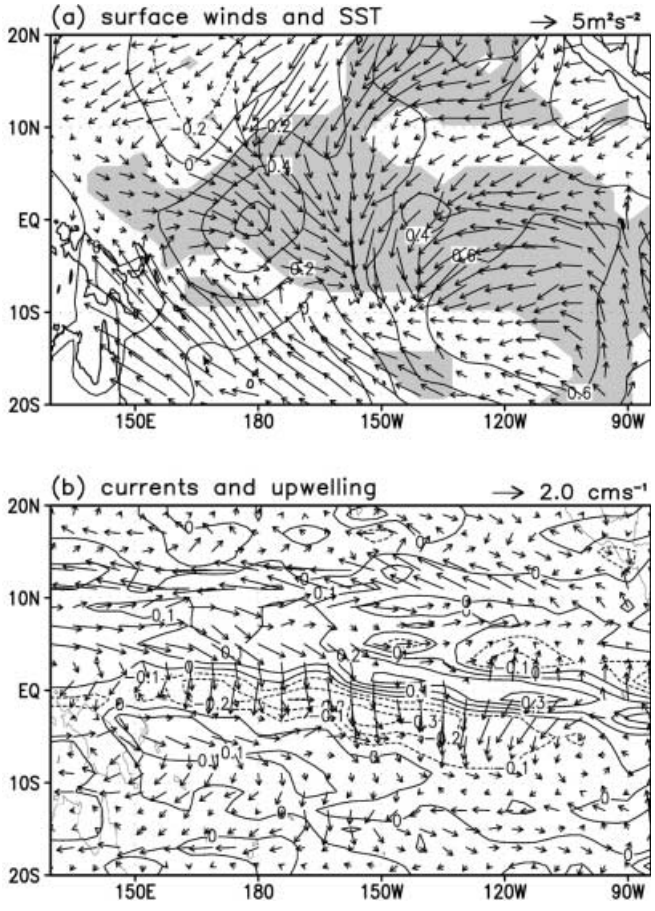

Fig. 2 **a** Differences in the annual mean pseudo wind stress (*vector*) and SST (contour interval is °C) between the 1961–1975 and 1981–1995 periods (the latter minus the former). The *shading* indicates areas where both wind stress and SST differences are significant at 5% confidence level by the two-tailed *t*-test. The *arrows* at the *upper right corner* of the figure give the scale for wind stress. The data used are the FSU wind stress and the NCEP reconstructed SST. **b** Same as in **a** except for the surface layer currents *(arrows)* and the upwelling (contour interval is 10^{-3} cm s^{-1}), which are obtained from the CZ ocean model forced by the observed surface wind stress

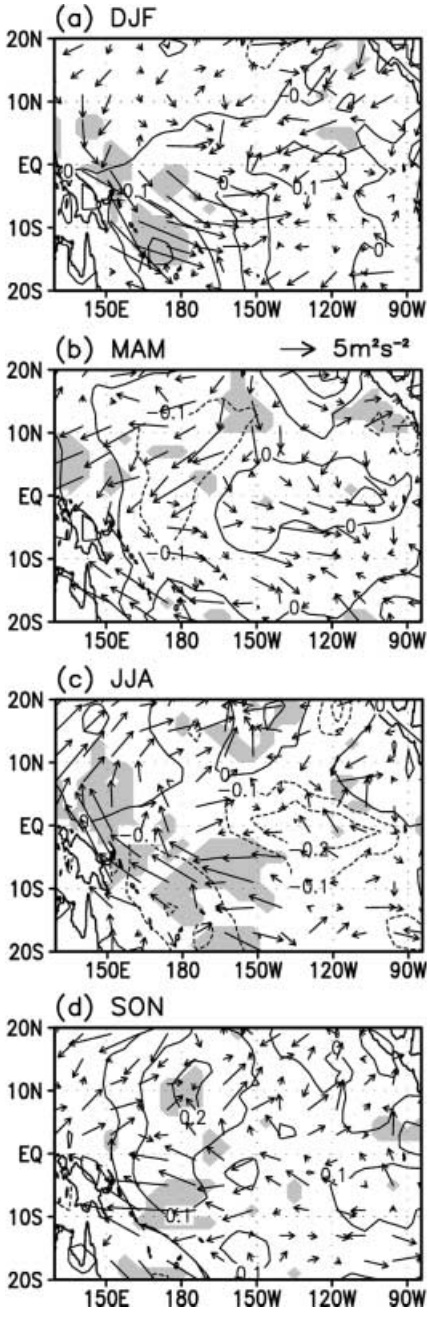

Fig. 3a–d Panels are the same as in Fig. 2a except for the four seasonal (DJF, MAM, JJA, SON) means, in which the annual mean is removed. The *shading* indicates areas where the wind stress or SST difference is significant at 5% confidence level by the two-tailed *t*-test

ocean, agreeing with the Matsuno (1966)-Gill (1980) solution for a steady atmospheric response to an enhanced convective heat source caused by a warm SST. This dynamical consistency derived from independent observations of surface winds and SST adds confidence to the detected decadal anomalies.

In correspondence to the changes in surface winds, the equatorial mean upwelling during the 1981–1995 period increased over the eastern Pacific (160°W-100°W) and decreased over the central Pacific (150°E-160°W) (Fig. 2b). Consistent with the wind change, near the equator, the eastward anomalous currents occur in the western Pacific while westward anomalous currents occur in the eastern Pacific, in consistence with the upwelling pattern.

The mean depths of the 20 °C isotherm (used as a surrogate to the equatorial thermocline depths) derived from the Levitus data (Levitus et al. 1994) for the two periods do not show appreciable differences (Fig. 4a). The changes in the vertical temperature gradient are also insignificant (Fig. 4b). Due to insufficient data coverage and crude vertical resolution of the observed subsurface temperature, the results here are considered suggestive. In Sect. 7, we will further discuss the uncertainties and difficulties in determining interdecadal changes in the mean thermocline depth and vertical temperature gradients.

Another empirical parameter used in the CZ model is the dependence of the subsurface temperature on the thermocline depth, which is represented by an empirical functional relationship between the thermocline depth h and the subsurface temperature T_{sub} (the temperature at 50 m depth), that is $T_{sub} = A \tanh(Bh)$. In the CZ model, the coefficients A and B depend also on the sign of the thermocline depth anomaly. For simplicity, here we calculated a representative value for the dependence of the subsurface temperature on the thermocline depth, $\gamma_o = AB\cosh^{-2}(Bh)$. Applying the least squares method, the two coefficients A and B for the two epochs were estimated from the Levitus data, where $h = 70$ m was used as an averaged value in the eastern half of the equatorial Pacific basin. The values of γ_o for the periods 1962–1975 and 1978–1990 are 0.145 °C $m^{-1}$and 0.152 °C m^{-1}, respectively, i.e., between the two periods, γ_o differs by about 5%. The model sensitivity test with a change of γ_o within 5% did not show a significant change in model ENSO.

In view of the uncertainty in decadal changes of the equatorial subsurface temperature field, we will disregard, in Sect. 4 through 6, the change in thermocline and focus on effects of the decadal changes in SST, surface winds and associated upwelling and currents on the ENSO properties. However, we will specifically discuss the effect of thermocline variation in Sect. 7.

4 Coupled model experiments

We adopted the CZ coupled anomaly model in which the basic states of the atmosphere and ocean are specified. The model describes essential ENSO physics, thus providing a convenient tool for identifying impacts of the basic states on ENSO and for understanding the causes. Numerical experiments were performed to examine possible changes in ENSO properties under the two sets of mean states, which were calculated using the procedures described in the previous section. Since the CZ model is sensitive to changes in the parameters, in order to maintain the model's coupled mode in an oscillatory regime and to keep the coupling coefficient unchanged, we specified the model basic state for the 1961–1975 (1981–1995) epoch by averaging the original CZ basic states and the observed basic state for the 1961–1975 (1981–1995) period. The resultant changes in the basic state are half of the observed changes between the two periods. For each experiment, the model was run for 1400 years and the statistical behavior of the model ENSO was examined using the model output from the last 1350 years.

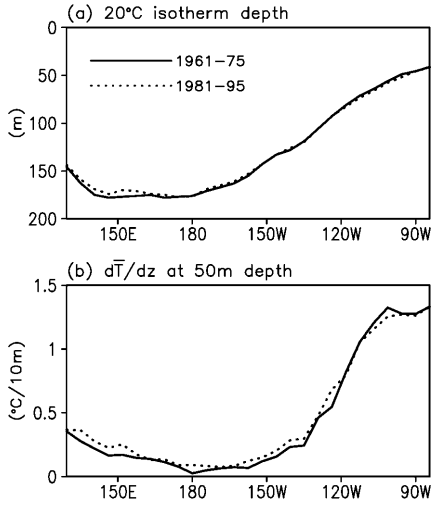

Fig. 4 **a** Annual mean 20 °C isotherm depth and **b** vertical temperature gradient $d\bar{T}/dz$ for the 1961–1975 (*solid line*) and 1981–1995 (*dotted line*) periods derived from Levitus (1994) ocean temperature data. The $d\bar{T}/dz$ at the bottom of the surface layer (50 m) was estimated using the temperature difference between 30 m and 75 m. The variables in **a** and **b** were averaged over the equatorial belt between 4.5°S and 4.5°N. Units in **a** and **b** are m and 0.1 °C m^{-1}, respectively

Figure 5 presents Nino-3 SST indices obtained from the experiments with two sets of basic state parameters representing the 1961–1975 and 1981–1995 periods, respectively. The model ENSO that was produced using the 1961–1975 basic-state has a relatively short period (about 3 years) and a moderate amplitude (the standard deviation of the Nino-3 SSTA appeared in Fig. 5a is 0.94 °C) (Fig. 5a). In contrast, the ENSO associated with the 1981–1995 basic-state exhibits a longer period (about 4 years) and larger amplitude (the standard deviation of the Nino-3 SSTA appeared in Fig. 5b is 1.32 °C) (Fig. 5b). Thus, the model results agree qualitatively well with the observed ENSO period and amplitude changes during the two periods (An and Jin 2000; An and Wang 2000).

To compare the structure of the dominant ENSO modes appearing in the two experiments, we applied the JSVD method to the anomalous SST, zonal wind stress, and thermocline depth fields. The JSVD modes for the first and second periods explain 94% and 95% of the total covariance, respectively. The spatial patterns of the most important JSVD mode resemble those derived from the assimilated data (Carton et al. 2000). The eastward shift of the anomalous westerly patch from the 1961–1975 to 1981-95 period is noticeable (Fig. 1b). This shift of the wind anomaly is accompanied by eastward shifts of the zonal SST gradient and the zonal gradient of the thermocline depth anomaly.

To display changes in the propagation characteristic of the model ENSO, we applied the space-time power spectral analysis (Hayashi 1977) to the anomalous SST along the equator, which yields both spectral density and propagation as a function of zonal wave number. As shown in Fig. 6, the higher-frequency westward propagating component is dominant when the 1961–1975 basic state is adopted, while the lower-frequency eastward propagating component is dominant in the experiment with the 1981–1995 basic state. These results are consistent with that observed (e.g., Wallace et al. 1998).

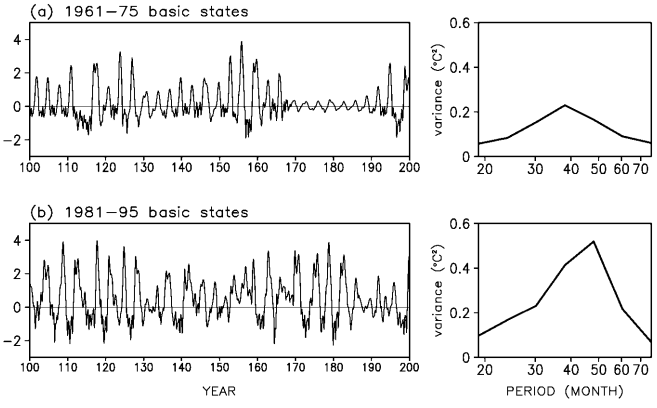

Fig. 5a,b Segments of time series of Nino-3 SST anomalies (°C) and the corresponding variance as a function of the oscillation period computed from the wavelet analysis of Nino-3 SST anomalies for a period of 1365-year model integrations. Results shown in panels (a) and (b) are obtained from benchmark experiments using the 1961–1975 and 1981–1995 basic states, respectively

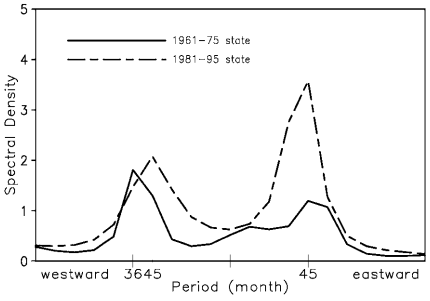

Fig. 6 The space-time power spectral density of the equatorial SST anomalies obtained from the CZ model benchmark experiments with the 1961–1975 basic state *(solid line)* and the 1981–1995 basic state *(dot-dashed line)*. The *left-* and *right-half* of the curves indicate the spectral densities associated with the westward- and eastward-propagating wave components, respectively

In summary, the behavior of the model ENSO obtained using the two sets of basic-state parameters were qualitatively consistent with the observed ENSO behavior in their frequency, amplitude, structure, and propagation, suggesting that the observed decadal changes in the frequency and the structure of ENSO mode are possibly caused by the interdecadal changes in the basic state SST and surface winds.

5 Principal factors contributing to the change of ENSO properties

As shown in Sect. 3, from 1961–1975 to 1981–1995 the changes in the annual mean are more significant than changes in the annual cycle. Are changes in the annual cycle unimportant? Motivated by this question, we first fix the basic states at the annual mean values for the two periods. The time series and corresponding power spectra obtained from the experiments with the 1961–1975 and 1981–1995 annual mean basic-states look alike (figure not shown). The dominant period is about 38 months for the 1961–1975 state and 39 months for the 1981–1995 state. The standard deviations are also comparable (1.47 °C and 1.67 °C, respectively). These results point out that the change of annual mean state alone was not able to modify the dominant frequency, although with the 1981–1995 state, the spectral power around the 6-year period is significantly increased. If the basic state annual cycles for the two periods are further added to the corresponding means, the model ENSO periodicity alters from 39 months during 1961–1975 to 50 months during 1981–1995 (Fig. 5a,b). However, this result does not mean that the change in the annual cycle is important. To elaborate on this point, we have taken the annual mean basic state parameters from the first (second) period and the annual departure from the second (first) period to make a "mixed" basic state. Examination of the response of the model ENSO reveals that for a given annual mean state, addition of an annual cycle of either the first or the second period yields a similar oscillation period (figure not shown). As far as the influence of the basic state is concerned, *the change of the annual cycle is not enough to change the model ENSO's characteristics, but the presence of an annual cycle of the basic state is necessary*. As shown in Sect. 3, the major changes of the mean state are found in SST and surface wind fields (including the associated wind divergence and ocean upwelling and surface layer currents). To further assess the relative roles of SST and surface winds, we performed the following two groups of sensitivity experiments.

In the first group, all basic state parameters are given the values of the 1961–1975 period (including both the annual mean and annual cycles) except that SST *or* surface winds (and associated oceanic fields) are given the value of 1981–1995 period. When only SST took the 1981–1995 state, the Nino-3 SSTA and the corresponding power spectrum representing the ENSO characteristics resembled those obtained using the 1961–1975 state, indicating that the change of the background state SST alone does not have a significant influence on model ENSO (figure not shown). On the other hand, when the basic state winds and the associated upwelling and surface layer currents were changed to the 1981–1995 values while all other parameters remained at the early epoch values, the model ENSO is similar to that obtained using the 1981–1995 basic states, implying that the changes in the surface winds and associated upwelling/currents are responsible for the changes in the model ENSO's period and amplitude.

In another group of experiments, all the basic state parameters are given the values for the 1981–1995 period except that SST or surface winds (and associated fields) which take the 1961–1975 mean values. Comparison of the resultant Nino-3 SSTA and the corresponding spectrum (not shown) confirms that the change in the basic state SST hardly influences model ENSO, whereas *changes in the basic state surface winds and the associated upwelling determine the oscillation period and amplitude*.

Although the basic state SST and surface winds can be separately specified in the model, in reality, they are coupled (Figs. 2 and 3). If the basic state winds are allowed to adjust to SST changes, the ENSO behavior could be indirectly affected by changes of the basic state SST. Since in the CZ model, the total SST controls the atmospheric heating, when SST and winds are artificially decoupled, the only way for the basic state SST to affect ENSO is through altering the convective heating. Thus, the results here indicate that the model ENSO is insensitive to effects of the background SST change on atmospheric heating.

6 Mechanisms responsible for the change of ENSO properties

6.1 How does the basic state change the structure of the ENSO mode?

The most significant change in the structure is an eastward displacement of the equatorial wind anomalies

during 1981–1995 (Fig. 1). One possible cause might be the dependence of the atmospheric heating on the basic state wind convergence. The heating in the CZ model depends on local SST anomalies (denoted by Q_s) and the low-level moisture convergence (denoted by Q_c) (Zebiak 1986). The former is regulated by basic state SST and the latter is affected by the surface wind convergence. We computed the Q_s and Q_c for the two sets of experiments. For clarity of comparison, the covariance between the normalized Nino-3 SST index and the two heating components along the equator is presented in Fig. 7. Evidently, for both epochs, the heating is primarily associated with the SST anomalies. For the period 1961–1975, Q_c is insignificant, but for the period 1981–1995, Q_c has a meaningful magnitude in the eastern Pacific, which makes the maximum of the total anomalous heating move eastward compared with the maximum Q_s. The increase of Q_c during 1981–1995 is a result of the increase in the mean surface convergence in the equatorial eastern Pacific as shown in Fig. 2a.

Another possible cause for the eastward shift of the wind anomalies might result from eastward displacement of the anomalous equatorial zonal SST gradients, because on the equator the surface zonal wind is determined by the boundary layer pressure gradient force that is induced by the zonal SST gradients (e.g., Lindzen and Nigam 1987; Wang and Li 1993). Figure 1 shows that the simulated zonal gradient of SST anomalies for the 1981–1995 epoch displays an eastward phase shift.

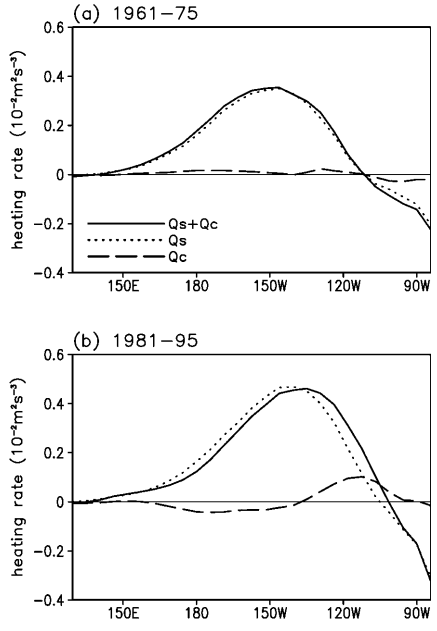

Fig. 7a,b Covariance between the normalized Nino-3 index and the local heating rate along the equator (*solid lines*) obtained from the CZ model using the **a** 1961–1975 and **b** 1981–1995 basic state parameters. The *dotted* and *dashed lines* denote, respectively, the covariance between the normalized Nino-3 index and the heating rate associated with the SST anomalies (Q_s) and the heating rate associated with the low-level moisture convergence (Q_c). Units are 10^{-2} m^2 s^{-3}

There is an increase of the positive SST gradient between 160°W and 110°W from the first to the second period (dotted lines in Fig. 8).

To unravel the causes of the eastward shift of the equatorial zonal SST gradient, we use the following flux form of the SST equation as a diagnostic tool:

$$\frac{\partial T'}{\partial t} = -u'\frac{\partial (T_m + T')}{\partial x} - v'\frac{\partial (T_m + T')}{\partial y} - \{M(w_m + w') - M(w_m)\}\frac{\partial (T_m + T')}{\partial z} - \frac{\partial (u_m T')}{\partial x} - \frac{\partial (v_m T')}{\partial y} - \frac{\partial (M(w_m)T')}{\partial z} - aT' \qquad (1)$$

Equation (1) was derived by combining the thermodynamic and the continuity equations. Kang et al. (2002) pointed out that Eq. (1) gives a more meaningful interpretation for SST budget. To assess the contribution of each process to the changes in zonal SST gradients, we took a partial derivative of Eq. (1) with respect to x. The resultant tendency equation for the zonal SST gradient is

$$\frac{\partial}{\partial t}\left(\frac{\partial T'}{\partial x}\right) = -\frac{\partial}{\partial x}\left(u'\frac{\partial (T_m + T')}{\partial x}\right) - \frac{\partial}{\partial x}\left(v'\frac{\partial (T_m + T')}{\partial y}\right) - \frac{\partial}{\partial x}\left(\{M(w_m + w') - M(w_m)\}\frac{\partial (T_m + T')}{\partial z}\right) - \frac{\partial}{\partial x}\left(\frac{\partial (u_m T')}{\partial x}\right) - \frac{\partial}{\partial x}\left(\frac{\partial (v_m T')}{\partial y}\right) - \frac{\partial}{\partial x}\left(\frac{\partial (M(w_m)T')}{\partial z}\right) - a\frac{\partial T'}{\partial x} \qquad (2)$$

The first three terms in the right hand side of Eq. (2) denote, respectively, effects of the zonal, meridional, and vertical advection of temperature by anomalous currents, and the fourth through sixth terms represent the influences of the anomalous zonal, meridional, vertical heat fluxes, respectively.

For convenience of comparison, we calculated the normalized covariance between the Nino-3 SST index and the tendency of zonal SST gradients associated with the first six terms in the right hand side of Eq. (2) for the 1961–1975 and 1981–1995 periods, respectively. The resultant covariance along the equator measures the contributions of each term to the tendency of zonal SST gradients. Figure 8 shows that the contribution of the anomalous vertical heat flux (Fig. 8e) and the anomalous vertical advection of the mean temperature (Fig. 8f) display a longitudinal distribution that is quite similar to that of the zonal SST gradient (dotted line in Fig. 8), suggesting that these two processes make a major contribution to the eastward shift of the zonal gradient of SST.

These two processes are related to the change of mean upwelling over the equatorial eastern Pacific. During 1981–1995, the maximum mean upwelling shifted east-

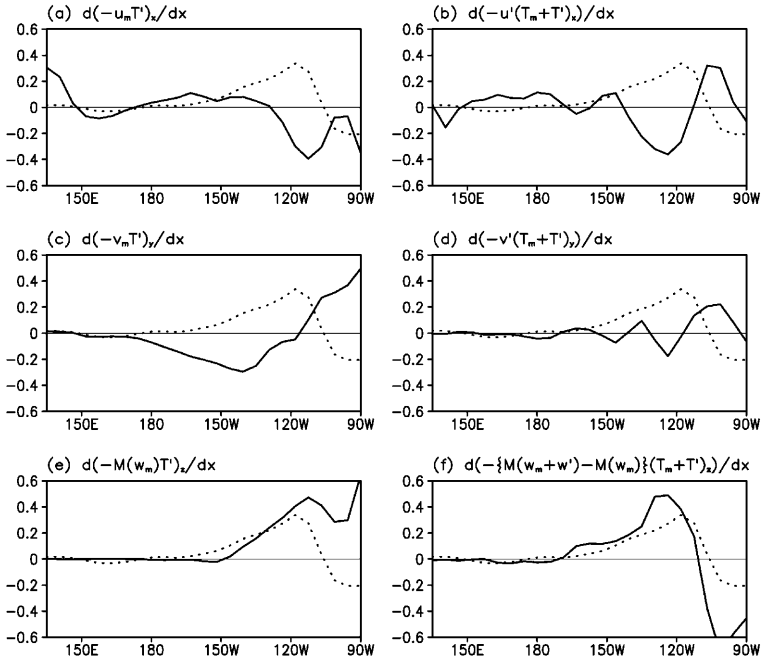

Fig. 8a–f Contribution of each term on the right hand side of Eq. (2) to the two-epoch difference (1981–1995 minus 1961–1975) in the zonal SST gradient tendency along the equator. The tendency terms are represented by the covariance between the normalized Nino-3 index and the local tendency of zonal SST gradient along the equator (averaged between 5°S and 5°N). The *dotted line* in **a** through **f** denotes the model simulated two-epoch difference in the equatorial zonal SST gradient. The units are 0.1 °C $(10^6\text{m})^{-1}$ month^{-1}

ward in the eastern-central Pacific in response to the change of the equatorial winds (Fig. 2b). Since the anomalous warming is associated with suppression of the mean upwelling, the eastward shift of mean upwelling implies a reduced warming in the central Pacific or an eastward shift of the maximum zonal SST gradient. In Sect. 5, we have identified that the change of surface winds, especially the equatorial winds, and associated upwelling play a critical role in changing ENSO behavior. The result here supports that assertion.

6.2 Why the ENSO frequency and amplitude changed

It is conceivable that the structural change may affect its oscillation amplitude and period. In fact, using a coupled model, which consists of the Cane-Zebiak ocean model and an idealized empirical atmosphere, An and Wang (2000) performed a series of experiments in which the longitudinal location of the wind response to SST can be artificially adjusted. The period of the model ENSO indeed lengthens when the westerly anomalies were displaced eastward relative to the eastern Pacific SST anomaly. Cane et al. (1990) also were dealing with the dependence of the frequency and growth rate on the position of the wind patch using their conceptual model, which showed a consistent result with those as in An and Wang (2000). According to the delayed oscillator theory (Suarez and Schopf 1988; Battisti and Hirst 1989), an eastward shift of the equatorial westerly anomalies would increase the distance over which the oceanic Rossby waves, which were generated by the equatorial wind anomalies, propagate before being reflected by the western boundary. Hence, the negative feedback of the reflected Rossby waves to the equatorial thermocline adjustment would be delayed. On the one hand, this delay allows for the positive wind-Kelvin wave-SST feedback to amplify the thermocline and SST anomalies in the eastern Pacific (Philander et al. 1984). On the other hand, the delay prolongs the turnaround period of the ENSO cycle. As a result, the ENSO cycle would have an increased amplitude and periodicity. This explains how the change of the structure of coupled mode leads to corresponding changes in the frequency and amplitude.

6.3 Why the propagation of SST anomalies changes

Propagation of SST anomalies depends primarily on competitive effects between vertical temperature advection, which supports eastward propagation, and the zonal temperature advection that promotes westward propagation (Fedorov and Philander 2000). This is because the anomalous thermocline depth and zonal current induced by wind stress forcing are primarily located to the east and west side of the wind fetch (An 2000). From the pre- to the post-shift period, the decrease of zonal mean SST gradient in the central-eastern Pacific and the increase of the eastern Pacific mean upwelling indicate that the effect of the vertical advection is enhanced while that of the zonal advection weakened (An and Jin 2000). As a result, the prevailing westward propagation was replaced by stationary or eastward propagation. Note that the decadal changes in vertical advection can be attributed to either the change in mean thermocline depth or the changes in the mean upwelling.

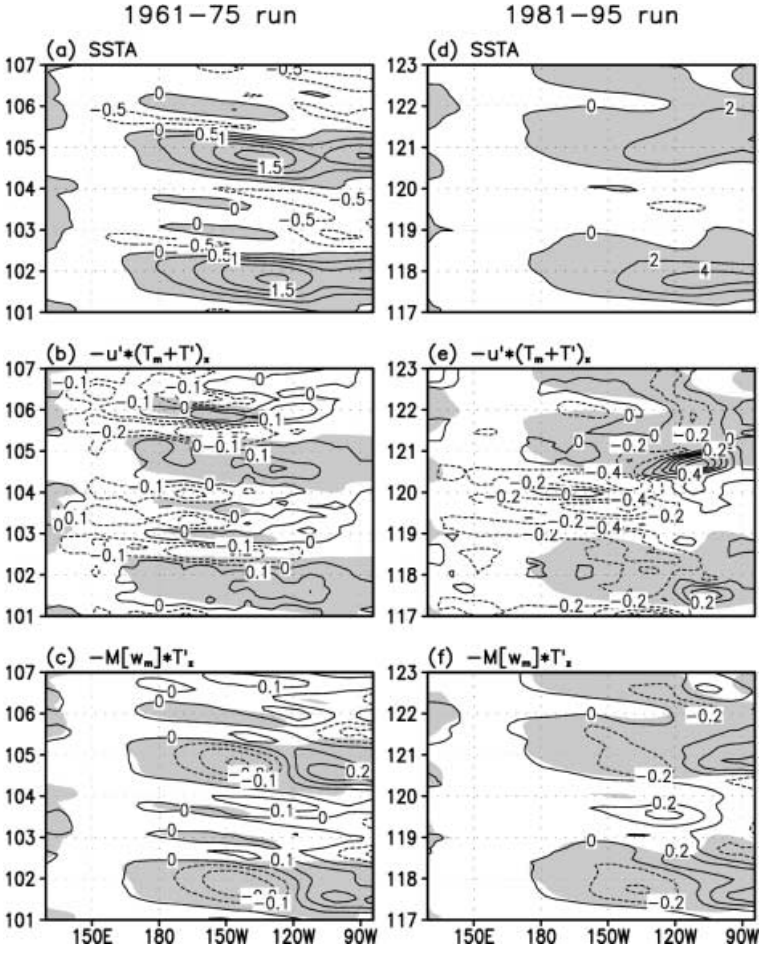

Fig. 9a–f Time-longitude diagram showing **a** SST anomalies, **b** temperature advection due to anomalous zonal current, and **c** vertical temperature advection by the mean upwelling. The data are obtained from the CZ model outputs using the 1961–1975 basic state. Panels **d–f** are the same as in **a–c**, respectively, except for the 1981–1995 basic state. The *shaded area* in each *panel* indicates the *positive* SST anomaly

Fedorov and Philander (2000) stressed the effect of the mean thermocline change, whereas we emphasize the effect of changing mean upwelling (Fig. 2b).

A direct comparison of the zonal and vertical advection in the CZ model experiments with two sets of basic state parameters also shows pronounced changes in their relative contributions. The SST advection due to anomalous zonal current in the pre-shift period expands from the eastern to the central Pacific, resembling the evolution of the warming (Fig. 9b), whereas that in the post-shift period it is localized in the eastern Pacific or shows a weak tendency of eastward propagation (Fig. 9e). In other words, the SST tendency due to the zonal temperature advection appeared in the pre-shift period (Fig. 9b) attributes to the prevailing westward propagation of SST anomalies, whereas that appeared in the post-shift period (Fig. 9e) favors a stationary mode or eastward propagation. The effects of changes of the vertical advection are not as obvious as that of the zonal advection, but in the 1961–1975 period a tendency of westward propagation can be seen in the eastern Pacific (Fig. 9c), while in the 1981–1995 experiment a tendency of eastward propagation can be found (Fig. 9f). The SST advection due to anomalous zonal current is more sensitive to the longitudinal migration of the wind stress anomalies than the vertical temperature advection by the mean upwelling.

7 Discussion

Due to the lack of long-term subsurface ocean data, particularly in the tropical central Pacific, it is extremely difficult to make a reliable estimate for the changes in the thermocline and subsurface temperature. Although the analysis of the Levitus data appears to suggest an insignificant change in the mean thermocline depth during the Pacific climate shift, the results are not conclusive. In addition, an abrupt shift in the coral record over a limited area of the tropical eastern Pacific since 1976 has been reported (Guilderson and Schrag 1998). For this reason, we have examined another subsurface temperature data set assimilated at the University of Maryland by Carton et al. (2000). Figure 10 shows a considerable discrepancy between the SODA and Levitus data sets. The SODA data show a rise of the thermocline primarily in the western equatorial Pacific after the climate shift. A part of the discrepancies between the Levitus and SODA data arise from the fact that the SODA model is forced by a de-trended wind stress field (Carton et al., 2000).

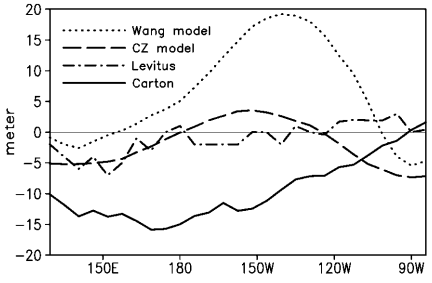

Fig. 10 The difference in the mean depth of the 20 °C isotherm between the 1961–1975 and 1981–1995 periods (the latter minus the former). The *solid* and *dot-dashed lines* denote the difference derived from the SODA data (Carton et al. 2000) and the Levitus (Levitus et al. 1994) data. The *dotted* and *dashed lines* denote thermocline depth difference between the 1961–1975 and 1981–1985 periods derived from the intermediate coupled model of Wang et al. (1995) and Cane and Zebiak (1985), respectively

Removal of long-term trends may have reduced the magnitude of the decadal variations in surface winds and affected the decadal variations in the thermocline. We have also taken the same wind forcing for the pre- and post-shift periods and forced two intermediate type ocean models (Zebiak and Cane 1987; Wang et al. 1995). The resulting thermocline depth differences between the two periods also differ substantially (Fig. 10).

Considering the uncertainty involved in the inter-decadal change in the thermocline depth, we assessed the sensitivity of ENSO behavior to the mean thermocline change in terms of idealized experiments, in which the mean thermocline is assumed to be uniformly raised or lowered across the entire equatorial domain. In a suite of experiments, the mean thermocline depth was progressively increased (or decreased) each by a 5-m interval. All other basic state parameters are kept unchanged. When the mean thermocline becomes too deep, the original CZ model failed to produce a sustained oscillation because of the reduced coupled instability. Since stochastic forcing was demonstrated to be able to excite and sustain ENSO modes in a stable regime of coupled ocean-atmospheric models (Chang et al. 1996; Wang et al. 1999), we added a random noise to the coupled system to mimic the effect of atmospheric transient forcing. This random noise was applied only to the zonal wind anomaly. The spatial structure of the stochastic forcing has a fixed elliptic shape with its long axis coincident with the equator and amplitude varying randomly with an upper limit of 0.2 m s^{-1}. All experiments were performed using the same type of stochastic forcing.

As the basic-state thermocline depth deviates from –15 m to +10 m, the dominant period, which corresponds to the maximum energy density peak, decreases systematically from about 5 years to 3 years (Fig. 11), indicating that a shallower basic-state thermocline favors a lower frequency ENSO. The results here imply that if the eastern Pacific thermocline had become shallower after the Pacific climate shift, the ENSO period could have increased accordingly. One cannot rule out this possibility.

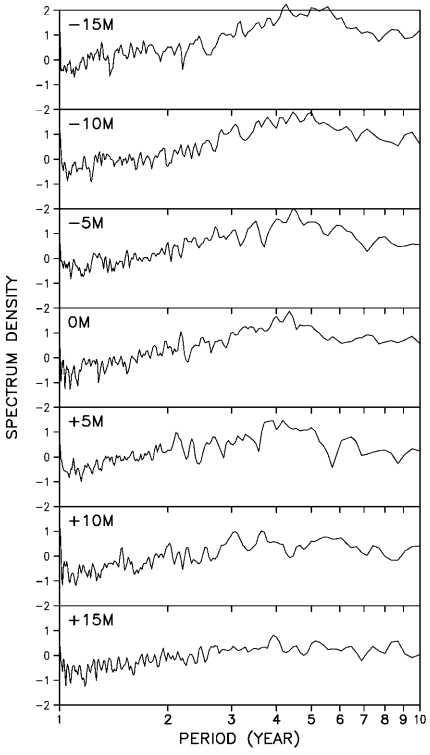

Fig. 11 Power spectra of the Nino-3 SST indices obtained from the CZ model experiments with modified mean thermocline depths. 0 M is the standard thermocline depth used in the original CZ model. –15 M, –10 M, ... denote mean thermocline depth anomaly. When the mean thermocline depth increases, the dominant spectral peak shifts to higher frequency

8 Summary

Comparison of the ENSO cycles observed during the 1961–1975 and 1981–1995 periods reveals that not only the amplitude and dominant period have increased but also the structure and propagation of the ENSO mode have changed since the late 1970s. A notable structural change of the coupled mode is an eastward displacement of the equatorial westerly anomalies (and associated anomalous thermocline slope) with respect to the eastern Pacific SST anomalies.

Using the Cane-Zebiak model, we demonstrate that the climate shift of the tropical Pacific background state in the late 1970s can result in changes in the oscillation period, amplitude, and the propagation and structure of the coupled ENSO mode that are all qualitatively similar to their observed counterparts. Sensitivity tests further reveal that while change in the long-term mean state is fundamental, the presence of the annual cycle is indispensable for the basic state to modulate ENSO. We identified that the principal factor that affected model ENSO behavior is the change in the basic-state equatorial winds and associated equatorial upwelling.

A novel explanation of the simultaneous and coherent changes of a number of ENSO characteristics is

offered. We explained why the changes in surface winds could modify the structure of the coupled mode, i.e., the eastward displacement of the equatorial westerly anomalies from the 1961–1975 to the 1981–1995 period. Two processes contribute to the eastward displacement of the westerly anomalies. First, during the 1981–1995 period, the increased mean trade wind convergence in the equatorial eastern Pacific favors an eastward shift of the anomalous atmospheric heating. Secondly, after the Pacific climate shift, the change of the background winds enhances the mean upwelling in the eastern Pacific while suppressing it in the central Pacific (Fig. 2b), resulting in an eastward shift of the maximum zonal SST gradient. The latter in turn facilitates eastward displacement of the equatorial westerly anomalies. We have shown that the structural change, in turn, amplifies the ENSO cycle and prolongs the oscillation period by enhancing the coupled instability and delaying transitions from a warm to a cold state or vice versa. The change of propagation of the SST anomalies is also a result of the changes in background winds. From the pre- to the post-shift period, the decrease of zonal mean SST gradients in the central-eastern Pacific and the increase of the mean upwelling in the eastern Pacific have amplified the role of the vertical advection (that promotes eastward propagation of SST anomalies) while reduced that of the zonal advection (that favors westward propagation). As a result, the prevailing westward propagation was replaced by stationary oscillation or eastward propagation.

Our model results emphasize critical roles of the atmospheric teleconnection, which could rapidly convey influences of extratropical decadal variations to ENSO through changing tropical winds and equatorial upwelling. We have detailed the processes by which the atmospheric teleconnection changes ENSO behavior, putting this hypothesis on a firmer physical ground. This new mechanism is appealing compared to the oceanic teleconnection hypothesis, because it explains why changes of ENSO behavior concur with the extratropical Pacific decadal variation.

Our model results also suggest the possibility that the Pacific climate shift might have affected ENSO properties by changing background tropical winds and the associated equatorial upwelling. This has implications to the possible changes of ENSO in a global warming scenario. In the event of a global warming, it is critical to know how increased greenhouse gasses would affect tropical winds, especially the equatorial winds. It is hoped that prediction of the change of ENSO properties can be achieved upon fully understanding the processes by which the background state influences ENSO.

In view of the simplicity of the model and the uncertainty of the observations, our model results are qualitatively indicative. The numerical experiments performed in this study are of an exploratory nature. In the present study, we have focused on the impacts of the basic state change on the behavior of ENSO and neglected the possible feedback of ENSO. However, the basic state we have derived from the observations already contains feedback effects of ENSO. The idealization introduced here amounts to that used in the study of baroclinic instability of an idealized basic state. Further study of the interaction between interdecadal variations of the mean state and the ENSO is required.

Acknowledgements This study is supported by NOAA OGP through Pacific Program and by Frontier Research System for Global Change through its sponsorship of the International Pacific Research Center. We thank Diane Henderson for her careful reading and editing of the manuscript. This is the School of Ocean and Earth Science and Technology publication Number 58/8 and International Pacific Research Center publication Number IPRC$_{-100}$.

References

An S-I (2000) On the slow mode of a simple air-sea coupled model: the sensitivity to the zonal phase difference between the SST and the atmospheric heating. J Meteorol Soc Jpn 78: 159–165

An S-I, Jin F-F (2000) An eigen analysis of the interdecadal changes in the structure and frequency of ENSO mode. Geophys Res Lett 27: 2573–2576

An S-I, Wang B (2000) Interdecadal change of the structure of the ENSO mode and its impact on the ENSO frequency. J Clim 13: 2044–2055

Anderson DLT, McCreary JP (1985) Slowly propagating disturbances in a coupled ocean-atmosphere model. J Atmos Sci 42: 615–629

Balmaseda MA, Davey K, Anderson DLT (1995) Decadal and seasonal dependence of ENSO prediction skill. J Clim 8: 2705–2715

Barnett TP, Pierce DW, Latif M, Dommenget D (1999) Interdecadal interactions between the tropics and midlatitudes in the Pacific basin. Geophys Res Lett 26: 615–618

Battisti SD, Hirst AC (1989) Interannual variability in the tropical atmosphere-ocean system: Influence of the basic state and ocean geometry. J Atmos Sci 46: 1678–1712

Cane MA, Munnich M, Zebiak SE (1990) A study of self-excited oscillation of the tropical ocean-atmosphere system. Part I: linear analysis. J Atmos Sci 47: 1562–1577

Carton JA, Chepurin G, Cao X, Giese B (2000) A simple ocean data assimilation analysis of the global upper ocean 1950-95. Part I: methodology. J Phys Oceanogr 30: 294–309

Chang CP, Ji L, Li H, Flugel M (1996) Chaotic dynamics versus stochastic processes in El Nino-Southern Oscillation in coupled ocean-atmosphere models. Physics D 98: 301–320

da Silva A, Young AC, Levitus S (1994) Atlas of Surface Marine Data 1994, NOAA Atlas NESDIS 6, US Department of Commerce, Washington, DC

Fedorov AV, Philander SGH (2000) Is El Nino changing? Science 228: 1997–2002

Gill AE (1980) Some simple solutions for heat-induced tropical circulation. Q J R Meteorol Soc 106: 447–462

Graham NE (1992) Decadal scale climate variability in the 1970s and 1980s: observations and model results: decadal-to-century time scales of climate variability. Academic, New York

Gu D, Philander SGH (1995) Secular changes of annual and interannual variability in the tropics during the past century. J Clim 8: 864–876

Gu D, Philander SGH (1997) Interdecadal climate fluctuations that depend on exchanges between the tropics and extratropics. Science 275: 805–807

Guilderson TP, Schrag DP (1998) Abrupt shift in subsurface temperatures in the tropical Pacific associated with changes in El Nino. Science 281: 240–243

Hayashi Y (1977) Space-time power spectral analysis using the maximum entropy method. J Meteorol Soc Jpn 55: 415–420

Kang I-S, Jin K, Wang, B, Lau K-M (2002) Intercomparison of the climatological variations of Asian summer monsoon precipitation simulated by 10 GCMs. Clim Dyn (in press)
Kirtman BP, Schopf PS (1998) Decadal variability in ENSO predictability and prediction. J Clim 11: 2804–2822
Kleeman R, Moore AM (1999) A new method for determining the reliability of dynamical ENSO prediction. Mon Weather Rev 127: 694–705
Kleeman R, McCreary JP, Klinger BA (1999) A mechanism for generating ENSO decadal variability. Geophys Res Lett 26: 1743–1746
Kubota M, O'Brien JJ (1988) Variability of the upper tropical Pacific Ocean model. J Geophys Res 93: 7155–7166
Latif M, Kleeman R, Eckert C (1997) Greenhouse warming, decadal variability, or El Niño? An attempt to understand the anomalous 1990s. J Clim 10: 2221–2239
Levitus S, Boyer T (1994) World Ocean Atlas 1994 vol 4: temperature. *NOAA Atlas NESDIS* **4**. US Department of Commerce, Washington, DC
Levitus S, Boyer TP, Antonov J (1994) World ocean atlas, vol 5: interannual variability of upper ocean thermal structure, *NOAA atlas NESDIS* **5**. US Government Printing Office, Washington, DC
Lindzen RS, Nigam S (1987) On the role of sea surface temperature gradients in forcing low-level winds and convergence in the tropics. J Atmos Sci 44: 2418–2436
Liu Z, Philander SGH, Pacanowski RC (1994) A GCM study of the tropical-subtropical upper ocean water exchange. J Phys Oceanog 24: 2606–2623
Matsuno T (1966) Quasi-geostrophic motions in equatorial areas. J Meteorol Soc Jpn 2: 25–43
McCreary JP, Lu P (1994) Interaction between the subtropical and equatorial ocean circulation: the subtropical cell. J Phys Oceanog 24: 466–497
Mitchell TP, Wallace JM (1996) ENSO seasonality: 1950-78 versus 1979-92. J Clim 9: 3149–3161
Nitta T, Yamada S (1989) Recent warming of tropical sea surface temperature and its relationship to the Northern Hemisphere circulation. J Meteorol Soc Jpn 67: 375–383
Nonaka M, Xie S-P, Takeuchi K (2000) Equatorward spreading of a passive tracer with application to North Pacific interdecadal temperature variations. J Oceanog 56: 173–183
Philander SGH, Yamagata T, Pacanowski RC (1984) Unstable air-sea interactions in the tropics. J Atmos Sci 41: 604–613
Pierce DW, Barnett TP, Latif M (2000) Connections between the Pacific ocean tropics and midlatitudes on decadal time scales. J Clim 13: 1173–1194
Rasmusson EM, Carpenter TH (1982) Variations in tropical sea surface temperature and surface wind fields associated with the Southern Oscillation/El Nino. Mon Weather Rev 110: 354–384
Reynolds RW, Smith TM (1994) Improved global sea surface temperature analysis using optimum interpolation. J Clim 7: 929–948
Schneider N, Venzke S, Miller AJ, Pierce DW, Barnett TP, Deser C, Latif M (1999) Pacific thermocline bridge revisited. Geophys Res Lett 26: 1329–1332
Shriver JF, O'Brien JJ (1995) Low-frequency variability of the equatorial Pacific ocean using a new pseudostress dataset: 1930-1989. J Clim 8: 2762–2786
Shukla J (1995) On the initiation and persistence of the Sahel drought. In: Natural climate variability on decade to century time scales. National Academy Press, Washington, DC, pp 44–48
Smith TM, Reynolds RW, Livezey RE, Stokes DC (1996) Reconstruction of historical sea surface temperature using empirical orthogonal functions. J Clim 9: 1403–1420
Suarez MJ, Schopf PS (1988) A delayed oscillator for ENSO. J Atmos Sci 45: 3283–3287
Trenberth KE (1990) Recent observed interdecadal climate changes in the Northern Hemisphere. Bull Am Meteord Soc 71: 988–993
Trenberth KE, Hurrell JW (1994) Decadal atmosphere-ocean variations in the Pacific. Clim Dyn 9: 303–319
Trenberth KE, Shea DJ (1987) On the evolution of the Southern Oscillation. Mon Weather Rev 115: 3078–3096
Troup AJ (1965) The Southern Oscillation. Q J R Meteorol Soc 91: 490–506
Wallace J, Rasmusson E, Mitchell T, Kousky V, Sarachik E, von Storch H (1998) On the structure and evolution of ENSO-related climate variability in the tropical Pacific: Lessons. J Geophy Res 103: 14241–14259
Wang B (1995) Interdecadal changes in El Nino onset in the last four decades. J Clim 8: 267–285
Wang B, Li T (1993) A simple atmospheric model of relevance to short-term climate variation. J Atmos Sci 50: 260–284
Wang B, Wang Y (1996) Temporal structure of the Southern Oscillation as revealed by waveform and wavelet analysis. J Clim 9: 1586–1598
Wang B, Li T, Chang P (1995) An intermediate model of the tropical Pacific Ocean. J Phys Oceanogr 25: 1599–1616
Wang B, Barcilon A, Fang Z (1999) Stochastic dynamics of El Nino-Southern Oscillation. J Atmos Sci 56: 5–23
Wang B, Wu R, Lukas R (2000a) Annual adjustment of the thermocline in the tropical Pacific Ocean. J Clim 13: 596–616
Wang B, Wu R, Lau K-M (2001b) Interannual variability of Asian summer monsoon: Contrast between the Indian and western North Pacific summer monsoons. J Clim 14:4073–4090
Zebiak SE (1986) Atmospheric convergence feedback in a simple model for El Nino. Mon Weather Rev 114: 1263–1271
Zebiak SE, Cane MA (1987) A model El Nino-Southern Oscillation. Mon Weather Rev 115: 2262–2278
Zebiak SE, Cane MA (1991) Natural climate variability in a coupled model. In: Schlesinger ME (ed) Greenhouse gas induced climate change. Elsevier, Amsterdam, pp 457–470
Zhang Y, Wallace JM, Battisti DS (1997) ENSO-like interdecadal variability: 1900-93. J Clim 10: 1004–1020